DOI: 10.1002/cctc.201100415

CHEMCATCHEM

ChemPubSoc Europe

DOI: 10.1002/cctc.201100415

Catalyst Recovery and Recycling Facilitated by Magnetic Separation: Iridium and Other Metal Nanoparticles

Marcos J. Jacinto,[a] Fernanda P. Silva,[a] Pedro K. Kiyohara,[b] Richard Landers,[c] and Liane M. Rossi*[a]

The immobilization of metal nanoparticles in magnetic responsive solids allows the easy, fast, and clean separation of catalysts; however, the efficiency of this separation process depends on a strong metal–support interaction. This interaction can be enhanced by functionalizing the support surface with amino groups. Our catalyst support contains an inner core of magnetite that enables the magnetic separation from liquid systems and an external surface of silica suitable for further modification with organosilanes. We report herein that a magnetically recoverable amino-functionalized support captured iridium species from liquid solutions and produced a highly active hydrogenation catalyst with negligible metal leaching. An analogous Ir^0 catalyst prepared with use of a nonfunctionalized support shows a higher degree of metal leaching into the liquid products. The catalytic performance in the hydrogenation of alkenes is compared with that of Rh and Pt catalysts.

Introduction

Iridium is a platinum group transition metal that is of particular interest for catalytic applications.[1] An iridium carbonyl catalytic system based on $Ir(CO)_xI_y$ species, Cativa, has shown many benefits over the conventional rhodium-based Monsanto technology used for methanol carbonylation in the production of acetic acid.[2] Bis(1,5-cyclooctadiene)iridium(I) complexes, also combined with a chiral ligand, are catalyst precursors for enantioselective hydrogenations, for example, the enantioselective hydrogenation of imines for the manufacture of (*S*)-metolachlor.[1] Well-known iridium complexes include Crabtree's catalyst,[3] a very active hydrogenation catalyst that is active even in the hydrogenation of sterically hindered alkenes, and Vaska's complex,[4] active in the decarbonylation of formate esters to form alcohols and CO.[5] Iridium in its reduced form $[Ir^0]_n$ has been less studied than other platinum group metal heterogeneous catalysts.[6] A limited number of research groups have synthesized, characterized, and explored the catalytic properties of Ir^0 nanoparticles in hydrogenation reactions in comparison to the extensive work on other platinum group metals, such as Pd, Pt, Rh, and Ru.[7] Moreover, if compared to the number of methodologies developed recently for the synthesis of other noble metal nanoparticles,[8] relatively few reports on the synthesis of different Ir^0 nanoparticles can be found in the literature.[7g,i,j,n,r,s,9] Despite its low availability,[1] the price of iridium is comparable to that of palladium as a result of its minor use in industry.[10] In addition, the straw-colored metal is not as commercially desirable on an aesthetic level as platinum, gold, and rhodium. Therefore, the development of better-quality particles for catalytic studies in the search for highly active Ir^0-based catalysts, as alternatives to noble metals of greater commercial interest, is of considerable significance.

Recent studies by our research team have focused on the design of noble metal nanoparticle catalysts supported on magnetic carriers,[11] seeking a fast and efficient method to separate products and catalysts in liquid phase batch reactions. Magnetic separation has attracted increasing interest in catalysis research.[12] The use of a magnetic separation tool simplifies greatly the workup and isolation of the desired product and makes the use of conventional separation methods, such as filtration and centrifugation, totally dispensable. Furthermore, product isolation can be completely achieved under solventless conditions. This is particularly important for laboratory-scale and batch reactions, in which the use of an extra solvent is commonly necessary. However, the efficiency of this separation process depends on a strong metal–support interaction, which can be enhanced by functionalizing the support surface with organosilanes.[13] Herein, we report the preparation of supported Ir^0 nanoparticles by in situ H_2 reduction of Ir^{3+} species bound to a catalyst support that contains an inner core of magnetite, which enables the magnetic separation from liquid systems, and an external surface of silica suitable for further modification with amino groups. The catalytic performance in the hydrogenation of alkenes is compared with that of Rh and Pt catalysts.

---

[a] *M. J. Jacinto, F. P. Silva, L. M. Rossi*
Instituto de Química
Universidade de São Paulo
Av. Prof. Lineu Prestes 748
05508-000 São Paulo (Brazil)
Fax: (+55) 11-38155579
E-mail: lrossi@iq.usp.br

[b] *P. K. Kiyohara*
Instituto de Física
Universidade de São Paulo
CP 66318, 05315-970 São Paulo (Brazil)

[c] *R. Landers*
Instituto de Física
UNICAMP
13083-970 Campinas (Brazil)

Results and Discussion

Catalytically active iridium(0) nanoparticles were prepared by reducing iridium trichloride, previously impregnated into the solid support, with hydrogen gas in liquid phase under mild conditions (100 °C and 6 atm H_2; 1 atm = 101.325 kPa). The preparation of Ir^0 nanoparticles is often accomplished by using organometallic precursors either by the hydrogen reduction of $[IrCl(cod)]_2$ (cod = 1,5-cyclooctadiene)[7b,d,f–h,m,n,q–s] or by the thermal decomposition of [(MeCp)Ir(cod)] (MeCp = methylcyclopentadienyl)[7j] and metal carbonyls $[Ir_4(CO)_{12}]$.[7a] The reduction of Ir^{3+} ions ($IrCl_3$) to zerovalent nanoparticles often requires stronger reducing agents, such as $NaBH_4$,[7i] or thermal treatment under reducing conditions.[14] We have shown here that Ir^0 nanoparticles can also be prepared by the reduction of iridium salts with hydrogen under mild conditions.

The core–shell catalyst support $Fe_3O_4@SiO_2$ obtained by means of a reverse microemulsion technique has been previously characterized[11c] and shows magnetic properties suitable for the easy separation of catalysts impregnated into it by using a permanent magnet and the immediate redispersion in liquid media for further use. This is possible because the magnetite core nanoparticles maintained the superparamagnetic behavior after receiving the silica shell. Any nonmagnetic material or molecules attached to the magnetic support in this regime can be separated by applying a remote magnetic field and are redispersed immediately after the field is removed. This separation process eliminates the use of any further physical or chemical procedure for catalyst isolation. With the use of this catalyst support we recovered, with high efficiency, Rh,[11e] Ru,[11c] Pt,[11d] and Pd[11b] nanoparticle catalysts after hydrogenation reactions.

The reaction with 3-aminopropytriethoxysilane provides an extra molecular silica layer enriched with NH_2 groups. The presence of these functional groups was characterized by means of X-ray photoelectron spectroscopy (XPS). In Figure 1, the N 1s spectrum could be deconvoluted into two peaks at 399.4 and 401.9 eV, which can be attributed to the primary amino group ($C{-}NH_2$) and its protonated $C{-}NH_3^+$ form, respectively.[15] This suggests an equilibrium of the protonated and deprotonated forms of the amino group on the surface of the solid, although the major component is still NH_2.

The first step in the catalyst preparation is the loading of the support with Ir^{3+} ions from aqueous solutions of iridium trichloride. The adsorption capacity of the prepared catalyst support is very low, and the presence of amino groups on the support surface was found to be important in increasing the metal uptake from aqueous solution (Figure 2 and Table 1). This behavior is similar to that observed for platinum[11d] and rhodium[11e] in our previous work with the same solid support. Moreover, we have suggested[11b] that the coordination of the metal ions to the organically modified support surfaces affects the nanoparticle formation, stabilization, and catalytic performance. Ir^0 nanoparticles could be easily prepared by the reduction of Ir^{3+} loaded into the support by H_2 under the conditions selected for the hydrogenation reactions. The material referred to as $Fe_3O_4@SiO_2{-}NH_2{-}Ir^{3+}$ (100 mg, 0.007 mmol Ir) was dispersed in cyclohexene (1.2 g, 14.6 mmol) and submitted to reduction in a glass reactor with H_2 (6 atm) at 100 °C. The reduction of $Ir^{3+} \rightarrow Ir^0$ promoted the hydrogenation of the substrate and was accompanied by a drop in the pressure in the H_2 supply tank connected to the main reactor. After the hydrogen consumption stopped, the hydrogenation reaction was complete (confirmed by use of GC) and a sample of the material, $Fe_3O_4@SiO_2{-}NH_2{-}Ir^0$, was collected and placed in a TEM grid for analysis. The catalyst morphology was assessed from the TEM micrographs.

The TEM image in Figure 3a reveals that the morphology of the catalyst support comprises a core–shell nanostructure of magnetite spherically coated with silica with an average size of

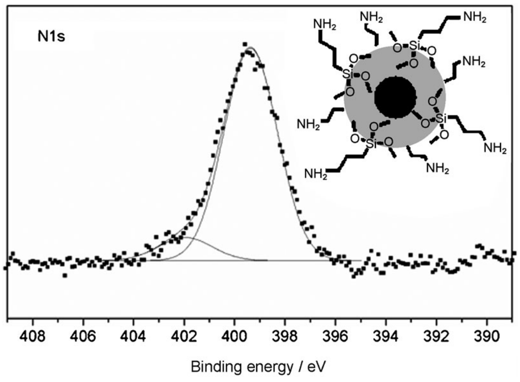

Figure 1. XPS spectrum of N 1s region of the amino-modified catalyst support ($Fe_3O_4@SiO_2{-}NH_2$).

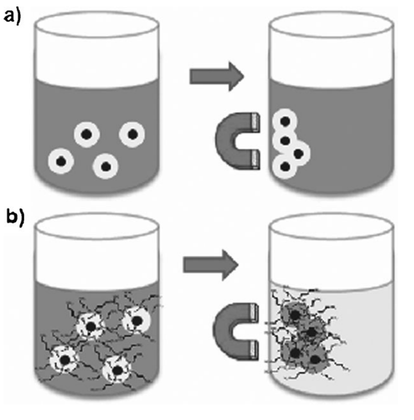

Figure 2. Metal impregnation into silica-coated magnetic supports by use of a) nonfunctionalized solids and b) amino-functionalized solids.

Table 1. Loading of iridium(III) ions into magnetic supports.[a]

Entry	Support	Metal loading[b] [wt %]
1	$Fe_3O_4@SiO_2{-}NH_2$	1.4
2	$Fe_3O_4@SiO_2$	0.17

[a] 100 mL of an aqueous solution containing iridium(III) chloride (1×10^{-3} mol L^{-1}) was added to 1 g of solid support; [b] Determined by ICP-OES.

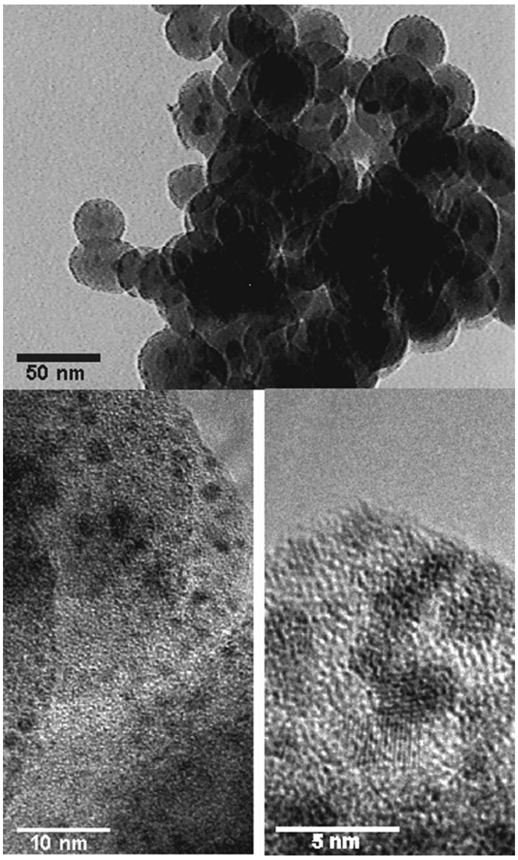

Figure 3. TEM analysis of the spent Ir^0 catalyst.

40–50 nm. However, the presence of iridium on the silica surface was confirmed only by use of energy-dispersive X-ray spectroscopy analysis. The analysis of high-resolution TEM micrographs such as those shown in Figures 3 b and c revealed Ir^0 nanoparticles of approximately 3–5 nm on the support surface. Surface analysis by XPS was used to verify the presence of iridium species on the support. The XPS analysis of the spent catalyst showed, as expected, the presence of iridium, silicon, and oxygen. The deconvoluted spectrum of the Ir 4 f level (Figure 4) exhibits two doublets that can be attributed to two chemically different Ir entities. The binding energy peaks at 61.4 and 64.4 eV can be assigned to the $4f_{7/2}$ and $4f_{5/2}$ peaks of metallic iridium, whereas the peaks at 62.7 and 65.7 eV can be assigned to the $4f_{7/2}$ and $4f_{5/2}$ peaks of iridium dioxide, which probably covers the Ir^0 nanoparticles.[7c,d]

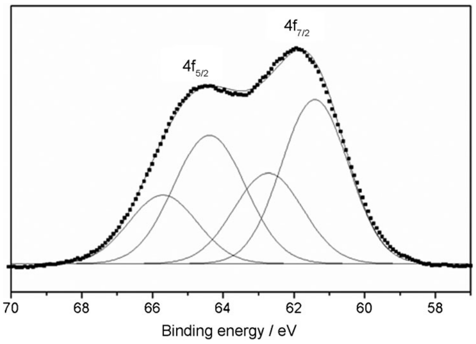

Figure 4. XPS spectrum of the 4 f region of the spent Ir^0 catalyst.

Table 2. Hydrogenation of cyclohexene by supported metal nanoparticles $Fe_3O_4@SiO_2-NH_2-M^0$.[a]

Entry	Catalyst	Olefin/metal molar ratio	t[b] [h]	TOF[c] [h^{-1}]	Reference
1	Ir	2000	0.33	6000	this study
2	Ir[d]	2000	0.28	7200	this study
3	Ir[e]	2000	0.36	5600	this study
4	Rh	1900	0.25	7600	[11e]
5	Ru	2100	5	420	[11c]
6	Pd	2500	0.45	5500	[11b]
7	Pt	1200	0.3	4000	[11d]

[a] Reaction conditions: constant hydrogen pressure (6 atm), solvent-free, 75 °C; [b] Time interval required for reaction completion estimated by H_2 consumption curves (>99 % conversion as determined by use of GC analysis); [c] Catalytic TOF: moles of substrate transformed per mole of catalyst (total metal) per hour at 100 % conversion; [d] First catalyst reuse; [e] Sixth catalyst reuse.

The magnetic-responsive supported Ir^0 catalyst was tested initially in the hydrogenation of cyclohexene (Table 2, entries 1–3). The results were obtained from a single portion of the catalyst used in successive hydrogenation reactions and separated exclusively by magnetic separation. After the first load of the substrate had been completely converted into cyclohexane [reaction time 0.33 h, turnover frequency (TOF) 6000 h^{-1}], the reactor was cooled to room temperature and the catalyst was separated magnetically by use of a permanent magnet that was placed on the glass reactor wall. After collecting the product by using a syringe, a new portion of the substrate was injected into the reactor and subjected to the same reaction conditions used in the first reaction. This method could be repeated up to six times with >99 % conversion and an accumulated turnover number of 12 600 mol of the substrate converted per mole of the catalyst (total metal) without catalyst deactivation. The performance of this catalyst is remarkable as compared to that of other Ir^0 nanoparticle catalysts tested in the hydrogenation of cyclohexene under similar conditions.[7s,a] It is also comparable to the performance of other metal catalysts prepared similarly by the hydrogen reduction of metal salts impregnated into the core–shell silica-coated magnetic nanoparticles (Table 2, entries 4–7). The general trend for the cyclohexene hydrogenation activity, comparing the TOF values estimated under similar conditions, of $Fe_3O_4@SiO_2-NH_2-M^0$-supported metals is $Rh > Ir > Pd > Pt \gg Ru$. This is only a rough comparison because the TOF values are estimated by using the total amount of metal and not the exposed metal atoms, which will vary according to the nanoparticle sizes. The data on the catalytic activity of the magnetically recovered Ir^0, Rh^0, and Pt^0 catalysts in the hydrogenation of other olefin compounds are summarized in Table 3. The highest TOF was observed for the less substituted nonaromatic alkenes. Moreover, double bonds conjugated to the aromatic ring are more difficult to reduce as can be seen in the ethenyl series and 2-propenylbenzene. The catalysts were active in the selective hydrogenation of the side chain of these substrates with >99 % conversion without touching the aromatic ring. Al-

Table 3. Hydrogenation of alkenes[a] by the Ir^0, Rh^0, and Pt^0 magnetic catalysts ($Fe_3O_4@SiO_2–NH_2–M^0$).

Entry	Substrate	Catalyst	t[b] [h]	TOF[c] [h^{-1}]
1	1-hexene	Ir	0.30	6666
2		Rh	0.08	15000
3		Pt[d]	0.10	12000
4	1-methylcyclohexene	Ir	3.04	675
5		Rh	0.29	4137
6		Pt[d]	0.35	3428
7	styrene	Ir	1.25	1600
8		Rh	0.23	5217
9		Pt[d]	0.27	4444
10	2-propenylbenzene	Ir	5.5	364
11		Rh	0.42	2857
12		Pt	n.d.	n.d.

[a] Reaction conditions: catalyst/substrate molar ratio 1:2000 (Ir) and 1:1200 (Rh and Pt), solventless, 75 °C, constant hydrogen pressure (6 atm); [b] Time interval required for reaction completion estimated by H_2 consumption curves and GC; [c] Catalytic TOF: moles of substrate transformed per mole of catalyst (total metal) per hour at 100% conversion; [d] Data from Ref. [11d].

though Rh^0 and Pt^0 are also active catalysts in the hydrogenation of aromatic bonds, the partially hydrogenated product could be isolated by stopping the reaction at the desired time after the inspection of the hydrogen consumption profile in hydrogenation curves. The difference between the reaction rates for the hydrogenation of olefinic and aromatic bonds is sufficient to distinguish between the two regimes and stop the reaction at the appropriate time (see also discussion in Ref. [11d]). Notably, the Ir^0 catalyst was inactive in terms of the additional reduction of aromatic bonds in these selected substrates under the conditions studied.

Additional experiments were conducted to identify whether the active catalysts behave as homogeneous or heterogeneous catalysts. No single technique can provide an unambiguous result; however, the association of different techniques can help to distinguish between the "homogeneous" and "heterogeneous" catalysts.[7m] These techniques include TEM studies, catalyst isolation studies, kinetic studies, and quantitative phenomenological studies with associated control experiments. In the TEM analysis (Figure 3), iridium nanoparticles with an average diameter of 3–5 nm were detected. The kinetic curve (Figure 5a) for the hydrogenation reactions has an induction period that evidences the in situ formation of the true catalyst by H_2 reduction of the Ir^{3+} precatalyst prior to the hydrogenation of the substrate. In the poisoning tests with elemental Hg (excess) and CS_2 (0.5 equiv.), the catalytic activity is immediately suppressed (Figures 5b and c). All the results suggest the presence of a heterogeneous Ir^0 catalyst. Moreover, the magnetic separation is very efficient and the products collected from the solventless hydrogenation of various substrates showed negligible Ir content in the organic phase [$Ir < 0.01$ ppm, by use of inductively coupled plasma optical emission spectroscopy (ICP-OES) analysis].

As previously mentioned, the presence of amino functional groups grafted onto the silica surface of the magnetic support improved the metal uptake in the catalyst preparation step. It is also reasonable to assume that the presence of these amino-binding sites increases the stability of the catalyst, avoiding metal leaching processes, a drawback associated with liquid phase reactions. Ir^0 catalysts prepared with the magnetic support, with and without surface functionalization, were brought into contact with polar substrates to test their stability. An example of the behavior observed by using different supports is shown in Figure 6. The Ir^0 catalyst immobilized in a nonfunctionalized solid could not be completely separated from anisole, and the total Ir leaching reached up to 22 ppm as compared to undectable levels of iridium achieved if the amino-functionalized solid support was used.

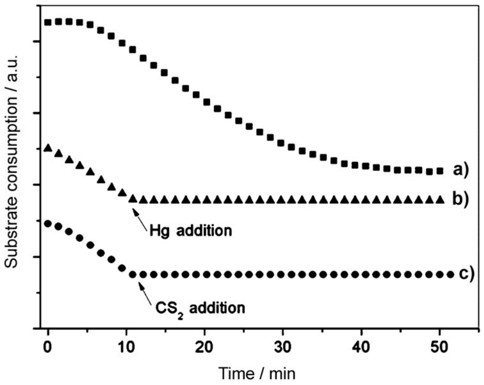

Figure 5. Hydrogenation of cyclohexene by supported Ir nanoparticles $Fe_3O_4@SiO_2–NH_2–Ir^0$: a) control experiment; b) poisoning experiment with Hg^0 (300 equiv.), and c) fractional poisoning experiment with CS_2 (0.5 equiv.).

Conclusions

An Ir^0 nanoparticle catalyst was prepared by the facile hydrogen reduction of Ir^{3+} loaded into an amino-modified silica support. No extra stabilizers or capping molecules were added to stabilize the particles in the range of 3–5 nm. The solid support contains a magnetic core that allows the quantitative recovery of the catalyst from the reactor wall by applying a permanent

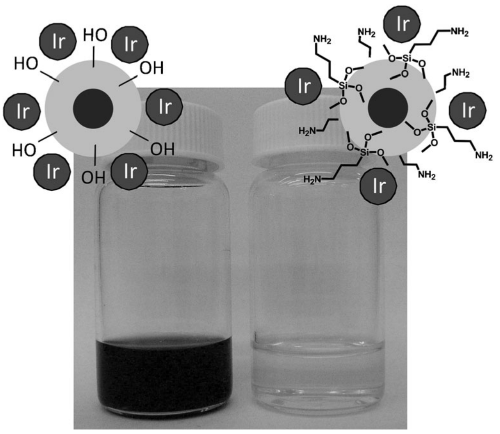

Figure 6. Supernatant solutions obtained after magnetic separation of Ir^0 catalysts immobilized on nonfunctionalized supports (left) and amino-functionalized supports (right) from anisole at room temperature.

magnet. The Ir^0 catalyst hydrogenates various alkene derivatives under mild conditions. Its catalytic performance was comparable to that of other platinum group metal catalysts prepared by our group—Rh > Ir > Pd > Pt ≫ Ru (cyclohexene hydrogenation at 75 °C and 6 atm H_2)—and superior to that of many other Ir^0 catalysts reported in the literature. In addition, an efficient recycling process using magnetic separation exclusively, with negligible metal loss, was obtained. Finally, the functionalization of the silica surfaces with amino groups improved the metal uptake and minimized metal leaching compared to nonmodified silica. The use of low metal concentrations, solventless conditions, mild pressure and temperature reactions, and solvent-free product isolation are important features of this "green" hydrogenation process.

Experimental Section

Preparation of the Ir^0 catalyst

The methodology used to prepare the catalyst support was based on the fabrication of $Fe_3O_4@SiO_2$, as reported elsewhere.[11e] A reverse microemulsion was prepared by adding the surfactant polyoxyethylene(5) isooctylphenyl ether (44.6 g), oleic acid-coated Fe_3O_4 (200 mg), and ammonium hydroxide (9.4 mL, 29 % commercial solution) to 700 mL of cyclohexane. The mixture was stirred until it became transparent. Then, tetraethylorthosilicate (7.70 mL) was added to the microemulsion. The solution was stirred gently for 16 h. The core–shell nanocomposite $Fe_3O_4@SiO_2$ (Brunauer–Emmett–Teller surface area = $69\ m^2 g^{-1}$)[16] was precipitated with methanol and collected by centrifugation at 7000 rpm. After the collected material was washed with ethanol, it was dried under vacuum, giving a yield of approximately 1 g.

The silica surfaces were further modified with amino groups by adding the dried solid to a toluene solution containing 3-aminopropyltriethoxysilane (200 mL, 1 % v/v solution in dry toluene) under N_2. The mixture was stirred for 2 h at room temperature, and then the amino-functionalized solid ($Fe_3O_4@SiO_2$–NH_2) was washed with toluene, separated by centrifugation, and dried for 20 h at 100 °C.

In the following step, the amino-functionalized magnetic solid $Fe_3O_4@SiO_2$–NH_2 (1 g) was added to an aqueous solution (100 mL) containing iridium(III) chloride ($1\times10^{-3}\ mol\,L^{-1}$). The mixture was stirred for 2 h at 25 °C. The solid was then magnetically collected and washed quickly with water and acetone and then dried at 100 °C for 3 h. The Ir^0 catalyst was prepared by in situ H_2 reduction (100 °C and 6 atm H_2) of the Ir^{3+}-loaded support dispersed in the substrate selected for the hydrogenation experiments. Similar experiments were performed with the nonfunctionalized solid ($Fe_3O_4@SiO_2$).

Catalytic reactions

The hydrogenation reactions were conducted in a modified Fischer–Porter glass reactor loaded with the supported Ir^{3+} catalyst precursor (100 mg, 0.007 mmol Ir) and the desired amount of liquid substrate (solventless conditions) under inert atmosphere. The reactor was connected to a pressurized H_2 tank through a gas regulator set to the required working pressure (typically 6 atm), which was maintained constant for the entire course of the reaction by leaving the reactor open to the H_2 supply tank. The temperature was maintained by using an oil bath and a hot-stirring plate connected to a digital controller (ETS-D4 IKA). The reactions were conducted under magnetic stirring (700 rpm). The fall in the H_2 pressure in the H_2 tank was monitored with a pressure transducer interfaced through a Novus Field Logger converter to a computer. The pressure versus time data were collected by the Field Chart Novus Software. After each reaction was complete, the catalyst was recovered magnetically by placing a magnet on the reactor wall and the products were collected and analyzed by use of GC and GC–MS. Samples of the Ir^0 catalyst were isolated through magnetic separation and dried under reduced pressure for TEM and XPS analyses. In the recycling experiments, the magnetically recovered catalyst was maintained inside the reactor and a new portion of the substrate was added under inert atmosphere. The reactor was connected again to the H_2 gas supply tank and successive hydrogenation reactions were performed.

Hg^0 and CS_2 poisoning test

The catalytic reactions were conducted under the same standard hydrogenation conditions, except for the addition of elemental Hg (300 equiv.) or CS_2 (0.5 equiv.) to the reaction mixture at 40 % conversion of cyclohexene to cyclohexane. The reaction was monitored by the fall in hydrogen pressure in the H_2 reservoir as a function of time before and after the addition of Hg or CS_2.

Catalyst characterization

TEM was performed at the Instituto de Física (IFUSP) on a Philips CM200 microscope operating at 200 kV. Samples for TEM observations were prepared by placing a drop containing the nanoparticles on a carbon-coated grid. High-resolution TEM was performed at the Laboratório Nacional de Luz Síncrotron (Campinas, Brazil) with a JEOL 3010 ARP microscope. The XPS spectra were obtained at the Instituto de Física (IF-UNICAMP) with a VSW HA-100 spherical analyzer using an aluminum anode (AlK_α line, $h\nu = 1486.6$ eV) X-ray source. The high-resolution spectra were measured with a constant analyzer pass energy of 44 eV, which produces a full width at half-maximum line width of 1.7 eV for the Au $4f_{7/2}$ line. The powdered samples were pressed into pellets and fixed to a stainless steel sample holder with a double-faced tape and analyzed without further preparation. To correct for charging effects, the spectra were shifted so that the C 1s binding energy was 284.6 eV. Curve fitting was performed by using Gaussian line shapes, and a Shirley-type background was subtracted from the data.

Acknowledgements

We are grateful to INCT-Catalise and the Brazilian government agencies FAPESP and CNPq for financial support. We also acknowledge Laboratório Nacional de Luz Síncrotron (Campinas, Brazil) for the use of high-resolution TEM facilities.

Keywords: hydrogenation · iridium · magnetic separation · nanoparticles · organosilanes

[1] P. B. Kettler, *Org. Process Res. Dev.* **2003**, *7*, 342 – 354.
[2] J. H. Jones, *Platinum Metals Rev.* **2000**, *44*, 94 – 105.
[3] R. Crabtree, *Acc. Chem. Res.* **1979**, *12*, 331 – 338.
[4] L. Vaska, J. W. Diluzio, *J. Am. Chem. Soc.* **1961**, *83*, 2784 – 2785.

[5] H. A. Zahalka, H. Alper, Y. Sasson, *Organometallics* **1986**, *5*, 2497 – 2499.
[6] M. D. Navalikhina, O. V. Krylov, *Kinet. Catal.* **2001**, *42*, 76 – 87.
[7] a) E. Redel, J. Kramer, R. Thomann, C. Janiak, *J. Organomet. Chem.* **2009**, *694*, 1069 – 1075; b) G. S. Fonseca, G. Machado, S. R. Teixeira, G. H. Fecher, J. Morais, M. C. M. Alves, J. Dupont, *J. Colloid Interface Sci.* **2006**, *301*, 193 – 204; c) G. Y. Fan, L. Zhang, H. Y. Fu, M. L. Yuan, R. X. Li, H. Chen, X. J. Li, *Catal. Commun.* **2010**, *11*, 451 – 455; d) I. S. Park, M. S. Kwon, K. Y. Kang, J. S. Lee, J. Park, *Adv. Synth. Catal.* **2007**, *349*, 2039 – 2047; e) P. Migowski, D. Zanchet, G. Machado, M. A. Gelesky, S. R. Teixeira, J. Dupont, *Phys. Chem. Chem. Phys.* **2010**, *12*, 6826 – 6833; f) G. S. Fonseca, J. B. Domingos, F. Nome, J. Dupont, *J. Mol. Catal. A-Chem.* **2006**, *248*, 10 – 16; g) G. S. Fonseca, J. D. Scholten, J. Dupont, *Synlett* **2004**, 1525 – 1528; h) G. S. Fonseca, A. P. Umpierre, P. F. P. Fichtner, S. R. Teixeira, J. Dupont, *Chem. Eur. J.* **2003**, *9*, 3263 – 3269; i) V. Mévellec, A. Roucoux, E. Ramirez, K. Philippot, B. Chaudret, *Adv. Synth. Catal.* **2004**, *346*, 72 – 76; j) C. A. Stowell, B. A. Korgel, *Nano Lett.* **2005**, *5*, 1203 – 1207; k) W. M. Alley, I. K. Hamdemir, Q. Wang, A. I. Frenkel, L. Li, J. C. Yang, L. D. Menard, R. G. Nuzzo, S. Özkar, K. A. Johnson, R. G. Finke, *Inorg. Chem.* **2010**, *49*, 8131 – 8147; l) E. Bayram, M. Zahmakiran, S. Özkar, R. G. Finke, *Langmuir* **2010**, *26*, 12455 – 12464; m) Y. Lin, R. G. Finke, *Inorg. Chem.* **1994**, *33*, 4891 – 4910; n) Y. Lin, R. G. Finke, *J. Am. Chem. Soc.* **1994**, *116*, 8335 – 8353; o) L. S. Ott, S. Campbell, K. R. Seddon, R. G. Finke, *Inorg. Chem.* **2007**, *46*, 10335 – 10344; p) S. Özkar, R. G. Finke, *J. Organomet. Chem.* **2004**, *689*, 493 – 501; q) S. Özkar, R. G. Finke, *J. Am. Chem. Soc.* **2005**, *127*, 4800 – 4808; r) M. A. Watzky, R. G. Finke, *Chem. Mater.* **1997**, *9*, 3083 – 3095; s) J. Dupont, G. S. Fonseca, A. P. Umpierre, P. F. P. Fichtner, S. R. Teixeira, *J. Am. Chem. Soc.* **2002**, *124*, 4228 – 4229.
[8] a) C.-J. Jia, F. Schueth, *Phys. Chem. Chem. Phys.* **2011**, *13*, 2457 – 2487; b) R. J. White, R. Luque, V. L. Budarin, J. H. Clark, D. J. Macquarrie, *Chem. Soc. Rev.* **2009**, *38*, 481 – 494; c) J. M. Campelo, D. Luna, R. Luque, J. M. Marinas, A. A. Romero, *ChemSusChem* **2009**, *2*, 18 – 45.
[9] a) P. S. Shah, S. Husain, K. P. Johnston, B. A. Korgel, *J. Phys. Chem. B* **2001**, *105*, 9433 – 9440; b) C. K. Yee, R. Jordan, A. Ulman, H. White, A. King, M. Rafailovich, J. Sokolov, *Langmuir* **1999**, *15*, 3486 – 3491.
[10] M. W. George, in *U.S. Geological Survey Mineral Commodity Summaries* (USGS Mineral Resources Program), **2008**.
[11] a) R. L. Oliveira, P. K. Kiyohara, L. M. Rossi, *Green Chem.* **2010**, *12*, 144 – 149; b) L. M. Rossi, I. M. Nangoi, N. J. S. Costa, *Inorg. Chem.* **2009**, *48*, 4640 – 4642; c) M. J. Jacinto, O. Santos, R. F. Jardim, R. Landers, L. M. Rossi, *Appl. Catal. A* **2009**, *360*, 177 – 182; d) M. J. Jacinto, R. Landers, L. M. Rossi, *Catal. Commun.* **2009**, *10*, 1971 – 1974; e) M. J. Jacinto, P. K. Kiyohara, S. H. Masunaga, R. F. Jardim, L. M. Rossi, *Appl. Catal. A* **2008**, *338*, 52 – 57.
[12] a) V. Polshettiwar, R. Luque, A. Fihri, H. Zhu, M. Bouhrara, J.-M. Bassett, *Chem. Rev.* **2011**, *111*, 3036 – 3075; b) Y. Zhu, L. P. Stubbs, F. Ho, R. Liu, C. P. Ship, J. A. Maguire, N. S. Hosmane, *ChemCatChem* **2010**, *2*, 365 – 374.
[13] R. L. Oliveira, D. Zanchet, P. K. Kiyohara, L. M. Rossi, *Chem. Eur. J.* **2011**, *17*, 4626 – 4631.
[14] S. Nassreddine, L. Massin, M. Aouine, C. Geantet, L. Piccolo, *J. Catal.* **2011**, *278*, 253 – 265.
[15] I. Roth, F. Simon, C. Bellmann, A. Seifert, S. Spange, *Chem. Mater.* **2006**, *18*, 4730 – 4739.
[16] F. P. Silva, M. J. Jacinto, R. Landers, L. M. Rossi, *Catal. Lett.* **2011**, *141*, 432 – 437.

Received: November 14, 2011
Revised: December 16, 2011